Published in final edited form as:
Adv Healthc Mater. 2014 April ; 3(4): 500–507. doi:10.1002/adhm.201300260.

Rapid and extensive collapse from electrically responsive macroporous hydrogels

Stephen Kennedy,
School of Engineering and Applied Sciences Harvard University, Cambridge, Massachusetts 02138, USA

Wyss Institute for Biologically Inspired Engineering Cambridge, Massachusetts 02138, USA)

Sidi Bencherif,
School of Engineering and Applied Sciences Harvard University, Cambridge, Massachusetts 02138, USA

Wyss Institute for Biologically Inspired Engineering Cambridge, Massachusetts 02138, USA)

Daniel Norton,
School of Engineering and Applied Sciences Harvard University, Cambridge, Massachusetts 02138, USA

Laura Weinstock,
School of Engineering and Applied Sciences Harvard University, Cambridge, Massachusetts 02138, USA

Manav Mehta, and
School of Engineering and Applied Sciences Harvard University, Cambridge, Massachusetts 02138, USA

Charité Medical School, Berlin 030 45050, Germany

David Mooney
School of Engineering and Applied Sciences Harvard University, Cambridge, Massachusetts 02138, USA

Wyss Institute for Biologically Inspired Engineering Cambridge, Massachusetts 02138, USA)

Stephen Kennedy: skennedy@seas.harvard.edu; David Mooney: mooneyd@seas.harvard.edu

Keywords

hydrogel; electroactive; stimuli responsive; drug delivery; tissue engineering

Electrically responsive hydrogels hold potential utility in numerous areas including robotic actuation, microfluidic control, sensory technology, optical devices, drug delivery, and

Correspondence to: Stephen Kennedy, skennedy@seas.harvard.edu; David Mooney, mooneyd@seas.harvard.edu.

Supporting Information
Supporting Information is available online from the Wiley Online Library or from the author.

tissue engineering.[1–4] These polyelectrolytic[1,2] hydrogels are of particular interest in applications that demand the material properties of hydrogels coupled with precisely timed, stimuli-proportioned control.[3–4] Indeed, their compatibility with electrical circuitry and microprocessor-based control systems provides great potential in coordinating complex actuations while using simple and inexpensive equipment. Despite this promise, electrically responsive hydrogels have been plagued by poor responsivity, precluding their use in many applications. A previous investigation[5] describes the electro-collapsibility of such polyelectrolytic hydrogels as a two-part process where an electric field exerts (i) a force on the charged polymer which draws the gel towards one electrode and (ii) an opposite force that draws mobile counterions towards the opposing electrode and out of the gel. Therefore, rapid hydrogel responsivity requires a design that enhances the movement of both water and ions in and through the hydrogel. The time required for water and ion diffusion can be reduced by simply scaling down the size of the hydrogels,[6] but this does not directly address the need to facilitate transport. Larger electrically responsive hydrogels have been limited to response times of 30 minutes[7], to hours[8,9,10], or tens of hours[5].

We hypothesized that gels with interconnected macroporous structures would allow for more efficient syneresis of water and egression of ions from the hydrogel, thus providing improved electrical responsivity. Additionally, apparent reductions in gel volume would be directly related to the volumetric collapse of macropores and not large-scale polymer matrix rearrangement *per se*. This would allow for more rapid reductions in gel volume while preserving the structural integrity of the gel. Finally, an interconnected macroporous structure would render the gel much softer, and therefore more electromechanically mutable. A cryopolymerization approach[11,12] (Supporting Information, Figure S1) was used to fabricate macroporous electrogels. Gels were formed in a semi-frozen state where nascent ice crystals concentrate monomer into the space between them, thus forming a concentrated gel structure interstitially between ice crystals following polymerization. When gels were thawed, ice crystals melted, leaving voids or pores. Cryogels fabricated from acrylic acid (AAc) and acrylamide (AAm) exhibited large, interconnected pores while gels formed at room temperature had no large pores (Figure 1a). The composition of the polymeric network influenced the macropore morphology. As total polymeric content increased, pores were generally more aligned and planar, but at the highest polymer concentrations the walls between pores became thicker. Quantification of gel properties confirmed that cryogels exhibited much higher degrees of pore interconnectivity (Figure 1b) and lower modulus (Figure 1c) than their room-temperature-polymerized, nanoporous counterparts. Note that at low overall polymer content, only cryogels were successfully formed. This is likely due to the increase in polymer concentration between ice crystals during cryotreatment. Macroporous cryogels were able to rapidly collapse to small diameters without loss of structural integrity when exposed to 50 V in deionized water, while nanoporous gels of the same makeup fragmented after about 30 seconds (Figure 1d). The ability to undergo large and rapid volumetric changes was associated with the transition of the cryogels' macropores from an open (Figure 1e, top) to a closed state (Figure 1e, bottom). While macroporosity may compromise potential utility in some applications (e.g., for use as valves), one can imagine straightforward ways to circumnavigate these compromises (e.g., using a macroporous gel as an actuator fixed to a nanoporous plug). The rapid and extensive

collapse observed here was primarily due to exposure to an electric field (estimated to be a radially graded field between 20-80 V cm^{-1}), with electrochemically induced changes in pH and ionic content having secondary roles (Supporting Information, Figure S2).

The electro-responsivity of these macroporous gels could be further enhanced by varying the concentration of charged polymer and net hydrogel charge. Gels were formed with different AAc concentrations while holding the bisacrylamide concentration constant at 0.1% wt, and gels composed of higher AAc concentrations generally collapsed slower and to a lesser extent (Figure 2a). However, quantification of the rate (Figure 2b) and extent (Figure 2c) of collapse revealed they did not monotonically vary with AAc concentration. For the 11% wt AAc gels, in particular, the rate of collapse significantly deviated from the trend. This likely resulted from the opposing effects of increasing the AAc concentration, in that it is expected to both (i) enhance responsivity by increasing the amount of charge in the gel (and therefore the amount of electromotive force exerted on the gel) (ii) reduce responsivity by increasing gel stiffness and impeding the movement of ions and water through the gel, and (iii) reduce responsivity by increasing the number of counterions required to translocate. Gels formed at 11% AAc likely balanced these three competing parameters to form a highly responsive gel. To examine the impact of polymer concentration independently of hydrogel charge content, cryogels were formed with both charged (AAc) and uncharged (AAm) monomers. The rate (Figure 2d, left graph) and extent (Figure 2d, right graph) of gel collapse over a wide range of AAc and AAm concentrations varied greatly. Note that while holding the AAm concentration constant, increasing the AAc concentration increases both the total polymer concentration and the hydrogel charge content. Just as observed with pure AAc gels (Figure 2b and c), at certain AAc concentrations the rate and degree of electrical collapse was optimized (Figure 2d, indicated by ⧦ at local minima), likely again through a balance of polymer concentration and charge content. Certain gel compositions exhibited better rates and degrees of collapse than the most responsive pure AAc gels (11%), as indicated by asterisks (Figure 2d). One gel formulation in particular (the 4% wt AAc, 4% wt AAm gel) outperformed the 11% wt AAc (0% AAm) gels in a statistically significant manner in regards to both rate *and* degree of collapse.

Surprisingly, the 4% wt AAc, 4% wt AAm gels (containing ~50% charged monomer, polymeric charge density of 0.007 $e\ Da^{-1}$) were more responsive than gels composed of lower charge densities. We attribute this to two possible phenomena: (i) utilization of more charged monomer increases the amount of counterions that need to be displaced before the gel can undergo volumetric collapse and (ii) an extremely high charge density along the polymer backbone results in more electrostatic repulsion between polymer chains, thereby impeding collapse. Indeed, previous studies have demonstrated electro-collapsiblity using polymeric charge densities lower than those of purely poly(AAc). AAc-*co*-AAm gels with a reported 20% charge along the polymer (0.0028 $e\ Da^{-1}$) were capable of extensive collapse (500-fold) but collapsed very slowly, likely due to their nanoporosity.[5] Relatively high temporal responsivities were reported (60% collapse in 30 minutes) when using nanoporous hyaluronic acid (HA) gels[7] (0.0026 $e\ Da^{-1}$). It has been shown previously that varying the polymer charge density alters responsivity, though responsivity was measured in terms of drug delivery and not explicitly by volumetric collapse.[13] Previously, drug delivery was

improved as charge density was increased from 0.0057 to 0.01 *e* Da^{-1}, [13] whereas we have found that responsivity (as measured directly by gel collapse) *worsens* as we increase charge density from 0.007 to 0.0139 *e* Da^{-1}. There are several specifics that may explain these different findings. First, we examined a slightly higher range in charge density. It is possible that electro-responsivity increases at relatively low charge densities (as examined by previously[13]) but decreases at higher charge densities (at the range we examined). This would be consistent with the aforementioned points (i) and (ii) in this paragraph. Second, the use of different metrics may have a substantial impact on results. When drug delivery is used as a metric of electro-responsivity,[13] electrostatic interactions between the drug, scaffold and electric field are in play.

The crosslinking density and the intensity of electrical stimulation had a dramatic impact on the dynamics of gel collapse. More highly cross-linked 4% wt AAc, 4% wt AAm gels had limited electro-responsivity, while gels with lower crosslinking densities collapsed faster and generally to a greater extent (Figure 3a). It has been shown previously that electro-responsivity is reduced at higher crosslinking ratios.[14] Here, varying the crosslinker from 0.1 to 0.5% wt was marked by a dramatic transition from nearly no to rapid electro-responsivity. Future studies are required to determine what crosslinking concentrations result in more moderate electro-responsivities. In the present study, even though the 0.01% and 0.1% wt BA gels performed similarly, the 0.1% wt BA crosslinked gels were used in subsequent experiments since the 0.01% wt BA gels often fragmented when handled. Application of higher voltages to the gels resulted in faster rates of collapse (Figure 3b), as seen in other reports.[15] However, increasing the voltage beyond 50 V only moderately enhanced the rate of collapse, suggesting that voltages lower than 50 V would be optimal, from the perspective of lower power consumption, less electrolysis, and the ability to regulate the rate of collapse in a voltage-proportioned manner. The proportioned but non-linear relationship between applied electrical stimulus and responsivity has been reported elsewhere,[16] and may be due to a maximum speed in which it takes counter ions to be electrophoretically removed from the gel.

The level of electro-responsivity provided by the 4 % wt AAc, 4% wt AAm, 0.1% wt BA cryogels when stimulated using 50 V is a marked improvement over the responsivity of similarly sized electrically collapsible hydrogels reported elsewhere. There have been several reports of similar or better electro-responsivites in micro-scale gels[6] and when characterizing responsivity based on hydrogel bending.[17,18,19] However, when comparing to gels of a similar size that experienced large-scale, voltage-dependent volumetric collapse, optimized cryogels were 40[7] to 2000[5] fold more electro-responsive. The performance of micro-scale gels could likely also be dramatically improved with the approach taken here. The ability of the electrogels described in this report to collapse so much more efficiently under electrical stimulus is likely a product of (i) a balanced charged to uncharged polymer ratio, (ii) a particularly organized and planar macroporous structure (Figure 1a), (iii) a relatively high pore interconnectivity (Figure 1b), and (iv) a relatively low modulus (Figure 1c).

These highly electro-responsive, macroporous gels were easily integrated into an optical array capable of configurational and chromatic modulation. Gels were created that contained

pigmented polystyrene beads and were placed in an array format (Figure 3c). This array of individually collapsible, pigment-containing gels was inspired by cephalopods, which are capable of modulating the optical profile of their skins using an array of collapsible pigment sacks called chromatophores.[20] Using this simple pigment sack configuration, cephalopods are able to rapidly camouflage themselves, optically blending into environments with both chromatic and textural complexities.[21] In our synthetic array, this optical adaptability was achieved simply by turning on the voltages addressed to particular gels. Both configurational ("H" in Figure 3c, top row) and chromatic (transition from red-blue-yellow to a primarily blue field in Figure 3c, bottom row) changes could be readily achieved. While these arrays do not achieve the spatiotemporal resolution provided by commercial optical display technologies (e.g., liquid crystal displays, plasma displays, cathode ray tubes), they do provide a means by which simple optical modulations can be achieved with hydrogels in aqueous environment using low amounts of energy, and unsophisticated and inexpensive electronics. This approach may be useful as adaptive camouflage, particularly in wet environments. A limitation, however, is that these gels take hours to re-swell back to their original size. When a reverse electric field was applied to a collapsed gel, the rate of reswelling was not enhanced. We think that during positive electric field excitation, collapse is favored since the gel is provided a surface about which to collapse (i.e., the center electrode) and the electric field intensity becomes more concentrated as the mass of the gel collects about the center electrode. However, with a reverse field, the gel is not anchored to the center electrode, is not provided a dense substrate against which to collect, and the field becomes less intense as the gel deswells radially outward.

Rapidly collapsible electro-responsive gels could also be made from biologically friendly materials, and were capable of efficiently harboring and delivering drugs when electrically stimulated in biological media. Macroporous gels containing AAc and crosslinked with 5 kDa poly(ethylene glycol) dimethacrylate (PEG-DM) were cryogelated, and exhibited the ability to electrically collapse (Figure 4a). The amount of anionic AAc and PEG-DM crosslinker used to form these electrogels had a deterministic effect on the rate (Figure 4b) and extent (Figure 4c) of electrical collapse. As observed in AAc-*co*-AAm gels (Figure 2b, c and d), increasing the amount of AAc—and therefore both the overall polymer concentration and total charge content—resulted in local minima at distinct AAc concentrations where polymer concentration and charge content were likely optimally balanced (indicated by ⧺ in Figure 4b). Out of these three gels, the 9% wt AAc, 1% wt PEG-DM gels were easiest to handle and did not fragment during preparation for experiments. These gels were loaded with mitoxantrone (Figure 4d, i)—an anthracenedion, antineoplastic drug used in the treatment of metastatic breast cancer, acute myeloid leukemia, non-Hodgkin's lymphoma,[22] and multiple sclerosis.[23] When not stimulated, these gels effectively retained drug, releasing drug at a rate of between 0.003-0.006 μg per minute (Figure 4d, vi). This corresponds to only 0.9-1.7% of the encapsulated drug being released per day. Subjecting gels held in phosphate buffered saline (PBS) to 2.5 V over the course of 15 minutes led to gel collapse (Figure 4d, ii-v). When gels were stimulated using two 2.5 V pulses lasting 10 minutes each (1 – 4 V cm^{-1} E-field, drawing < 5 mW power), the drug delivery rate was enhanced by 450- to 1800-fold, with release rates ranging from 2.7-5.4 μg min^{-1} (5.4-10.8% of encapsulated drug released in only 10 minutes). Note, however, that

only the first pulse resulted in a statistically significant increase in drug release. The large error bars are likely the result of the cryopolymerization process, where there is a wide variation in gel structure and surface area. Refinement of the cryopolymerization process or adoption of alternative means of generating macropores likely would improve these results. Interestingly, the drug delivery rate could roughly be doubled by increasing the applied voltage two-fold, resulting in a 1300- to 6000-fold enhancement in drug delivery rate (Supporting Information, Figure S3). The amount of drug delivery could also be regulated by the duration of electrical stimulation, though not linearly so, as the amount of drug release tapers off during stimulation (Supporting Information, Figure S4).

Compared to previously reported electrically collapsible drug delivery hydrogels,[13–15, 24–25] our gels provided heightened performance, particularly in terms of the degree to which drug release was enhanced when electrically stimulated (1000s-fold vs. two- to five-fold[13–15, 24–25] enhancement). The dramatic increase in drug release rate was likely due to both convective (via volumetric collapse) and electrophoretic (electrically stripping drug away from the scaffold) mechanisms, while the excellent retention was likely due to drug-scaffold electrostatic affinity. Affinity-based drug approaches from hydrogels have previously proven to provide a means by which the drug delivery profile can be tuned *a priori* while using gel fabrication techniques that preserved macromolecular bioactivity.[26] Our approach expands upon these advantages by additionally providing on-demand, stimuli-proportioned control.

Complex delivery profiles of multiple drugs were achieved by integrating these drug-containing gels into an array format. In a 10-gel array (Figure 4e, top image), five gels containing Auramine O were assigned to voltage v_1 and triggered from 0-30 minutes. Two gels containing mitoxantrone were assigned to v_2, and triggered from 60–70 minutes and then again from 120–130 minutes. The remaining three mitoxantrone-loaded gels were assigned to v_3 and triggered from 120–130 min. The timing and rate of release for both drugs were controlled by the timing and location of voltage applied to the distinct voltage addresses (Figure 4e, bottom graph). An initial burst of Auramine O (i; 0 to 30 minutes) was obtained by triggering the five gels containing this drug to collapse over this time frame. A subsequent period during which no voltage was applied to any gels (ii; 30 to 60 minutes) resulted in little drug release. Subsequently triggering the two gels assigned to v_2 (iii; 60–70 minutes), resulted in a small burst in mitoxantrone release. A period of little drug release (iv; 70 to 120 minutes) again followed, during which no voltage was applied. Finally, a relatively large burst in mitoxantrone release was obtained by simultaneously triggering the second collapse of the two gels assigned to v_2, and the collapse of the last set of gels assigned to v_3 (v; 120 to 130 minutes). The slight amounts of Auramine O release in the second and third drug delivery phases are likely a result of Auramine O's weaker electrostatic interaction with the poly(AAc) matrix. The act of retrieving the sample from and adding fresh PBS to the device results in a small amount of Auramine O release, particularly since the prolonged electric field exposure during the first 30 minutes of experimentation likely liberated a great deal of Auramine O from within the gels. It is also possible that small local changes in pH during subsequent electrical stimulations (i.e., v_2 and v_3) may also influence Auramine O release. Reservoir-based, microchip drug delivery arrays

have been used to similarly coordinate the delivery of multiple drugs;[27] however, these microchip-based systems assume very different physical forms than the system described here. Additionally, the recent demonstration that drug release can be triggered using a wireless system in human subjects[28] supports the potential utility of electrically responsive cryogels. While previously described reservoir systems have enormous potential, they have not demonstrated the ability to coordinate the delivery *rate* of multiple drugs through stimuli proportioned control, but instead demonstrate all or nothing release from a reservoir. The system we have shown here is capable of stimuli proportioned regulation (Supporting Information, Figure S3). This ability to coordinate the release rates of multiple drugs may be crucial in applications such as detoxification, pain relief, vaccination, infection combat, cancer treatment, diabetes treatment, the treatment of degenerative diseases (e.g., Alzheimer's and Parkinson's diseases), tissue engineering, and even in non-biomedical areas.[29] These arrayed electrically responsive hydrogels may also aid in understanding and better controlling the highly choreographed sequence of events associated with tissue development and regeneration.[30]

In sum, macroporous hydrogels have been made using an inexpensive, straightforward, and scalable process, and exhibited dramatically improved electo-responsivity in terms of the rate, degree and quality of volumetric collapse. These cryogels electrically collapsed 63% in 25 seconds and 93% in 150s, corresponding to a 40-2000 fold improvement over previous reports. Electrogels were easily integrated into arrays capable of simple and rapid configurational and chromatic optical modulations, and when loaded with drugs, were able to coordinate the release profile of multiple drugs with great flexibility. Further, they exhibited efficient stimulated delivery (6000-fold increase in delivery rate at 5 V). Enhanced performance of these electrogels will likely expand their utility in optics and drug delivery and will facilitate their use in a variety of other emerging technologies.

Experimental Section

Hydrogel and cryogel preparation

To form nanoporous PAAc-co-AAm hydrogels, depending on hydrogel composition, different amounts of Acrylic Acid (AAc), Acrylamide (AAm), NaOH (at 465 μg per mg of AAc), Bisacrylamide (BA), deionized water, and pigment (methacrylated rhodamine or polystyrene beads) were mixed by vortexing. Then, Tetramethylethylenediamine (TEMED) and Ammonium Persulfate (APS) redox reagents were added and the solution was transferred to room-temperature Teflon molds (¾ inch diameter, 2 mm thick) for gelation in 600 μl aliquots. After 1 hour, hydrogels were transferred to deionized water and allowed to fully swell overnight. They were rinsed three times in deionized water and cut to 19 mm diameter disks prior to experimentation. All chemicals, reagents and polymers were purchased from Sigma-Aldrich Corp., St. Louis MO., USA.

PAAc–*co*-AAm cryogels were formed in a similar fashion except using frozen Teflon molds. After mixing and addition of redox reagents, cryogel precursor solutions were transferred to frozen Teflon molds in a -20°C freezer and left to gel at -20°C overnight (see Supporting Information, Figure S1a for an illustration of the cryogelation process). This extended overnight gelation time was required as the rate of APS radical generation is

greatly reduced at low temperatures. This slower rate of gelation was in fact advantageous, as the cryopolymerization approach requires that ice crystals form *before* gelation. Gels were then removed from the freezer, thawed, and transferred to a petri dish containing deionized water where they were allowed to fully swell for one day. They were rinsed three times in deionized water and cut to 19 mm diameter disks prior to experimentation. Repeat experiments were performed using gels cast in independent molds.

PAAc-*co*-PEGDM cryogels were fabricated in a similar manner as the PAAc–*co*-AAm cryogels. For drug delivery experiments, after cryopolymerization, they were removed from the freezer, thawed and allowed to swell overnight in Phosphate Buffered Saline (PBS) containing 1 mg ml^{-1} of drug (i.e., either mitoxantrone or Auramine O). They were cut to 19 mm diameter disks and rinsed in PBS once prior to experimentation.

Evaluation of electro-responsivity

Nanoporous hydrogels and macroporous cryogels (19 mm diameter disks) were transferred to a custom electric-field exposure device (schematic and photographs in Supporting Information, Figure S1b and c). This device exposed the hydrogel samples to outward radial electric fields (Supporting Information, Figure S1b) that were proportional in magnitude to the voltages applied across the device's stainless steel electrodes. The gels were submerged in 150 mL of either deionized water or PBS, depending on the experiment. A voltage source was connected to the electrodes that was capable of providing up to 1000 VDC. Gel diameters during the course of 10 minute experiments were monitored (Supporting Information, Figure S1c). Photographs were taken from a stationary camera and these photographs were used to either (i) plot the hydrogel diameter vs. time, (ii) determine the time at which gel diameter becomes 50% of its original diameter (Supporting Information, Figure S1c, middle right image), and/or (iii) determine the hydrogel diameter at 10 minutes (Supporting Information, Figure S1c, bottom right image). Gels collapsed primarily radially with very little variation in gel thickness during electrical exposure since, as intended, the electric field did not vary significantly in the *z*-direction.

Evaluation of drug release

For all drug delivery experiments, drugs were loaded by rehydrating the gel in concentrated drug-containing PBS following cryopolymerization. It was estimated that gels contained roughly 750 μg of each drug. For experiments where only mitoxantrone release was quantified, custom vials were made from Teflon, where19 mm diameter gels could be exposed to voltages while being submerged in 15 ml of PBS (Figure 4d, i-v). During drug release studies, samples of the PBS/drug could be removed from the vials intermittently and analyzed for mitoxantrone content. This was done by measuring optical absorbance of the samples at 610 nm and using a linear regression standard curve generated with known drug quantities to correlate the amount of optical absorbance to mitoxantrone concentration values.

In experiments where multiple drugs were released from 10-gel arrays, a custom array-formatted device (Figure 4e) was made from Teflon, where ten 19 mm diameter gels could be exposed to ten independent voltages, allowing gels to be triggered individually or in

concert. All ten gels were submerged in 50 ml of PBS. During experimentation, gels would release their drug into the same 50 mL PBS basin. Samples of PBS/drug could be removed from the device's basin intermittently and analyzed for mitoxantron and auramine O content simultaneously. This was done by measuring optical absorbances at 610 nm (corrected at 640 nm) for mitoxantrone and 410 nm (corrected at 370 nm) for auramine O. Individual mitoxantrone and auramine O standard curves were used to correlate the optical absorbances at 610 nm and 410 nm to mitoxantrone and auramine O concentrations, respectively.

Supplementary Material

Refer to Web version on PubMed Central for supplementary material.

Acknowledgments

This work was supported by grants from the National Institutes of Health (NIH) (2 R01 DE013349) and the Defense Advanced Research Projects Agency (DARPA) (W911NF-10-0113) (DM). Support was also provided by the National Science Foundation's Research Experiences for Undergraduates (REU) program (NSF DMR-1005022) (LW). The microCT images presented in this work were taken and analyzed at Harvard University's Center for Nanoscale Systems (CNS). The authors would like to thank Louis DeFeo and his team at the Harvard School of Engineering and Applied Sciences Scientific Instrumentation and Machine Shop for their help with building the hardware used in this work. Finally, the authors would like to thank Kevin Parker, David Clarke, Zhigang Suo and Evelyn Hu for the many thoughtful conversations, insights and feedback provided during the course of this research.

References

1. Chidsey CED, Murray RW. Science. 1986; 231:25. [PubMed: 17819225]
2. Calvert P. MRS Bull. 2008; 33:207.
3. Murdan S. J. Control. Release. 2003; 92:1. [PubMed: 14499181]
4. Bar-Cohen Y, Zhang Q. MRS Bull. 2008; 33:173.
5. Tanaka T, Nishio I, Sunm ST, Ueno-Nisho S. Science. 1982; 218:467. [PubMed: 17808541]
6. Beebe DJ, Moore JS, Bauer JM, Yu W, Liu RH, Devadoss C, Jo CB-H. Nature. 2000; 404:588. [PubMed: 10766238]
7. Tomer R, Dimitrijevic D, Florence AT. J. Control. Release. 1995; 33:405.
8. Sutani K, Kaetsu I, Uchida K. Radiat. Phys. Chem. 2001; 61:49.
9. Yang Y, Engberts J. Coll. Surf. A: Physiocochem. Eng. Aspects. 2001; 169:85.
10. Murdan S. J. Control. Release. 2003; 92:1. [PubMed: 14499181]
11. Bencherif SA, Sands WR, Bhatta D, Arany P, Verbeke C, Edwards DA, Mooney DJ. Proc. Natl. Acad. Sci. USA. 2012; 109:19590. [PubMed: 23150549]
12. Kumar A, Srivastava A. Nat. Protoc. 2010; 5:1737. [PubMed: 21030950]
13. Yuk SH, Cho S, Lee HB. Pharm. Res. 1992; 9:995.
14. Paradee N, Sirivat A, Naiamlang S, Prissanroon-Ouajai W. J. Mater. Sci: Mater. Med. 2012; 23:999. [PubMed: 22354328]
15. Sawahata K, Hara M, Yasunaga H, Osada Y. J. Control. Release. 1990; 14:253.
16. Kwon C, Bae YH, Okano T, Kim SW. J. Control. Release. 1991; 17:149.
17. Osada Y, Okuzaki H, Hori H. Nature. 1992; 355:242.
18. O'Grady ML, Kuo P, Parker KK. ACS Appl. Mater. Interfaces. 2010; 2:343. [PubMed: 20356178]
19. Shiga T, Kurauchi T. J. Appl. Polym. Sci. 1990; 39:2305.
20. Mäthger LM, Hanlon RT. Cell Tissue Res. 2007; 329:179. [PubMed: 17410381]
21. Hanlon, RT.; Chiao, CC.; Mathger, LM.; Buresch, KC.; Barbosa, A.; Allen, JJ.; Siemann, L.; Chubb, C. Animal camouflage: mechanisms and functions. Stevens, M.; Merilaita, S., editors. Cambridge, United Kingdom: Cambridge University Press; 2011. Ch. 9

22. Parker C, Waters R, Leighton C, Hancock J, Sutton R, Moorman AV, Ancliff P, Morgan M, Goulden N, Green N, Révész T, Darbyshire P, Love S, Saha V. Lancet. 2010; 376:2009. [PubMed: 21131038]
23. Fox E. Clin. Ther. 2006; 28:461. [PubMed: 16750460]
24. Niamlang S, Sirivat A. Int. J. Pharm. 2009; 371:126. [PubMed: 19162150]
25. Juntanon K, Niamlang S, Rujiravanit R, Sirivat A. Int. J. Pharm. 2008; 356:1. [PubMed: 18242901]
26. Vulic K, Shoichet MS. J. Am. Chem. Soc. 2012; 134:882. [PubMed: 22201513]
27. Santini JT, Cima MJ, Langer RA. Nature. 1999; 397
28. Farra R, Sheppard NF, McCabe L, Neer RM, Anderson JM, Santini JT, Cima MJ, Langer RA. Sci. Transl. Med. 2012; 4:1.
29. Langer RA. Science. 1990; 249:1527. [PubMed: 2218494]
30. Reichert WM, Ranter BD, Anderson J, Coury A, Hoffman AS, Laurencin CT, Tirrell D. J. Biomed. Mater Res. Part A. 2010; 96:275.

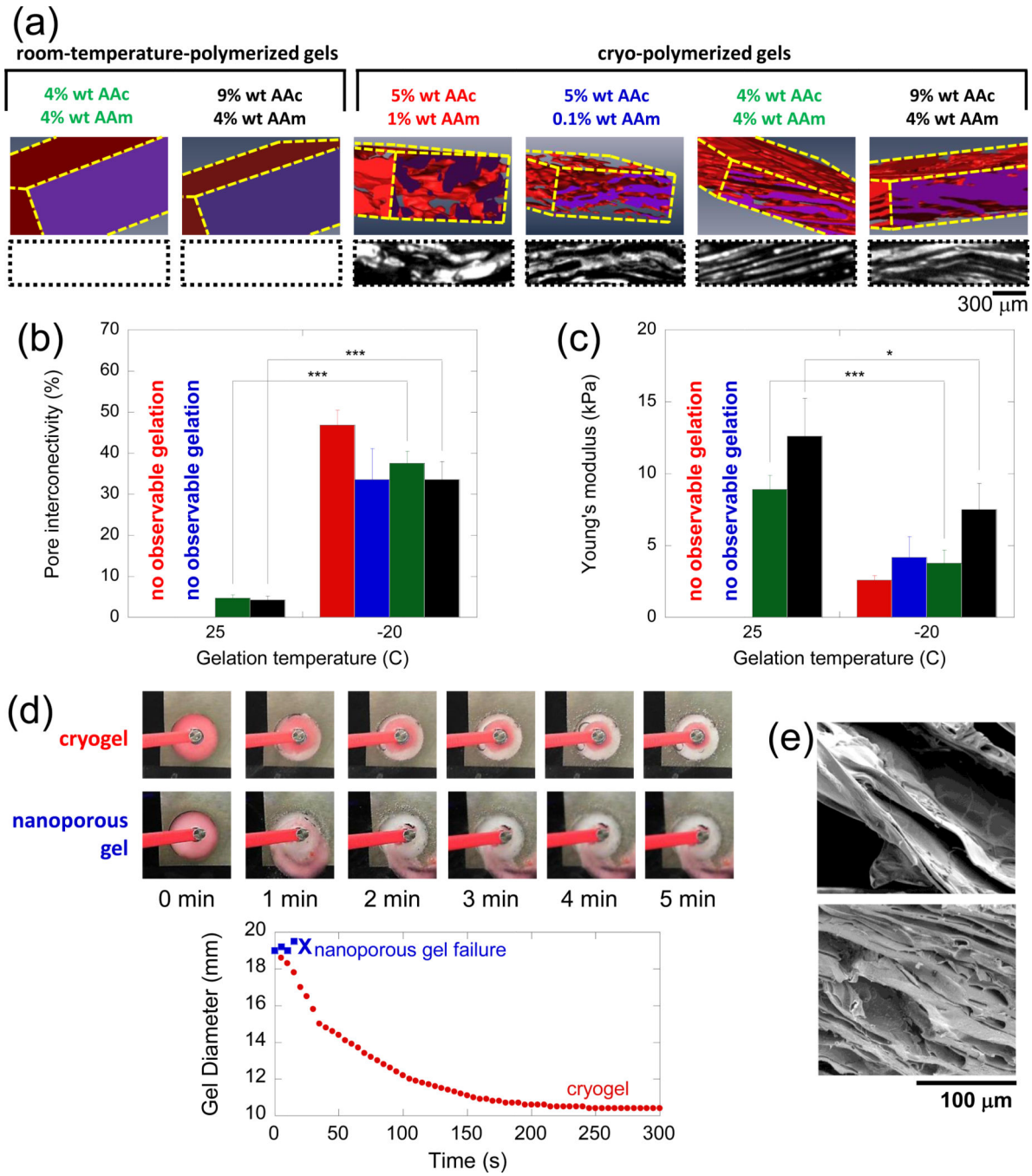

Figure 1.

Macroporous gels exhibit increased porosity and are able to collapse more rapidly and to a greater extent than their room-temperature-gelled counterparts. a) X-ray microtomography 3D reconstructions (top row) and cross-sections (bottom row, black space represents macropore space) compare the porosity of select room-temperature and cryo-polymerized gels. All gels were crosslinked using 0.1% wt BA. Pore interconnectivity as measured by water wicking method (b) and Young's moduli (c) are compared for the gels shown in part (a): gel composition is indicated by bar graph color, as referenced in part (a). (d) Time

course snapshots (top) and diameter versus time plot (bottom graph) comparing gel collapse for a nanoporous and cryogel of the same polymeric makeup. (e) SEM images of the cryogels, highlighting their pore structure before (top) and after (bottom) electrical collapse. In (b) and (c), values represent mean and standard deviation (N = 6). *, **, and *** indicate $p \leq 0.05$, 0.01, and 0.001, respectively.

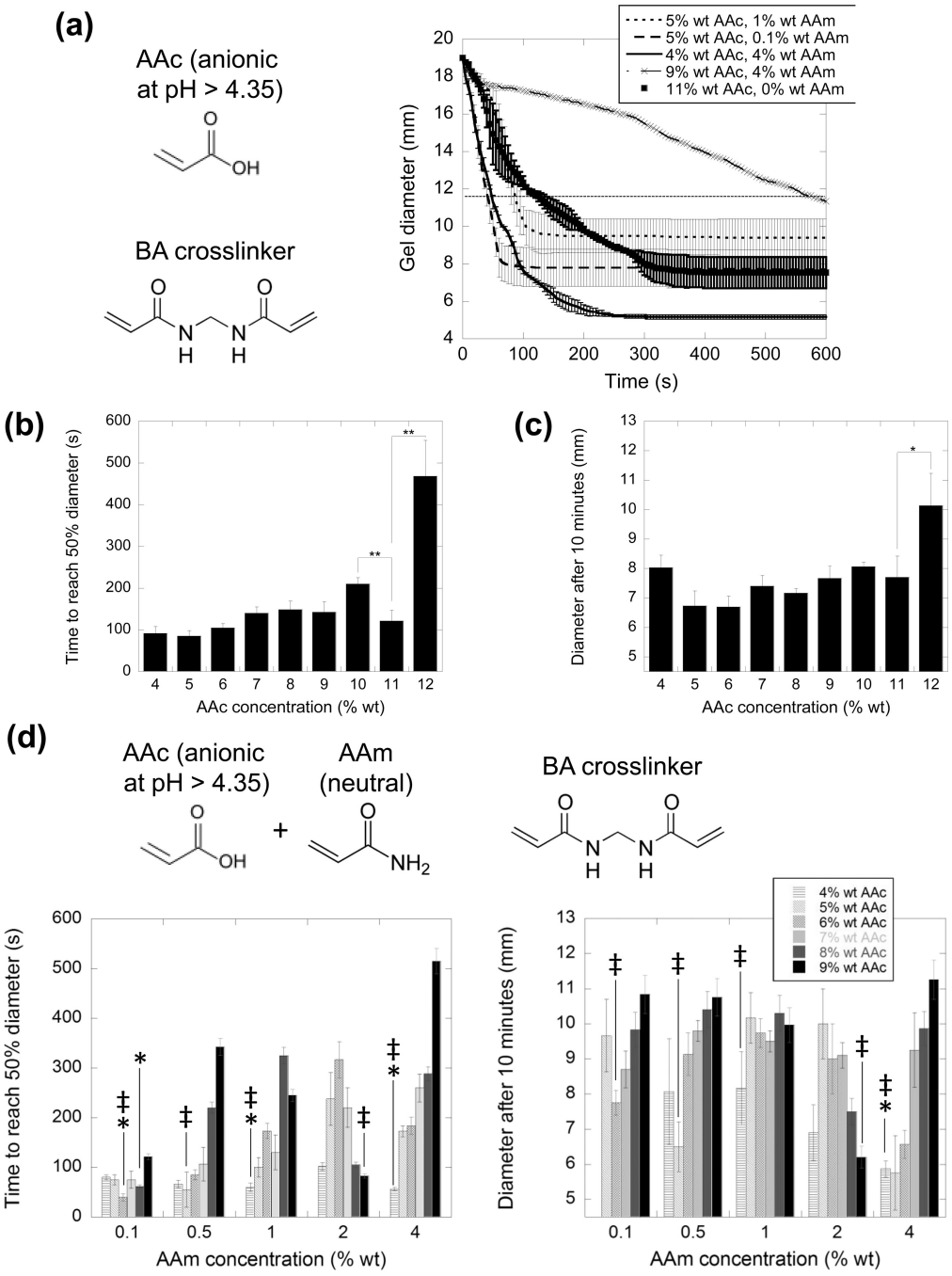

Figure 2.

The rate and extent of electrical collapse depends on the hydrogel polymer type and amount. a) Gel diameter versus time for samples at the indicated AAc and AAm concentrations. The horizontal black line represents the half-diameter of the gel (half way between the maximum gel diameter of 19 mm and its minimum possible diameter of 4.5 mm). The time it takes gels to reach half diameter (b) and the diameter of the gels after 10 minutes (c) are plotted for gels over a range of AAc concentrations. d) The time to reach half diameter (left graph) and diameters after 10 min (right graph) are plotted for gels composed of both AAc (anionic)

and AAm (neutral) at the indicated concentrations. In (a) through (d), all gels were crosslinked using 0.1% wt BA, had initial diameters 19 mm, and were exposed to 50 V in deionized water. All values represent mean and standard deviation (N = 3). * and ** indicate $p \leq 0.05$ and 0.01, respectively. In (d) ⫫ represent gels identified as having enhanced electro-responsivity. Asterisks signify that values are statistically less than the corresponding values of the 11% wt (0% wt AAm) gels in parts (a), (b) and (c).

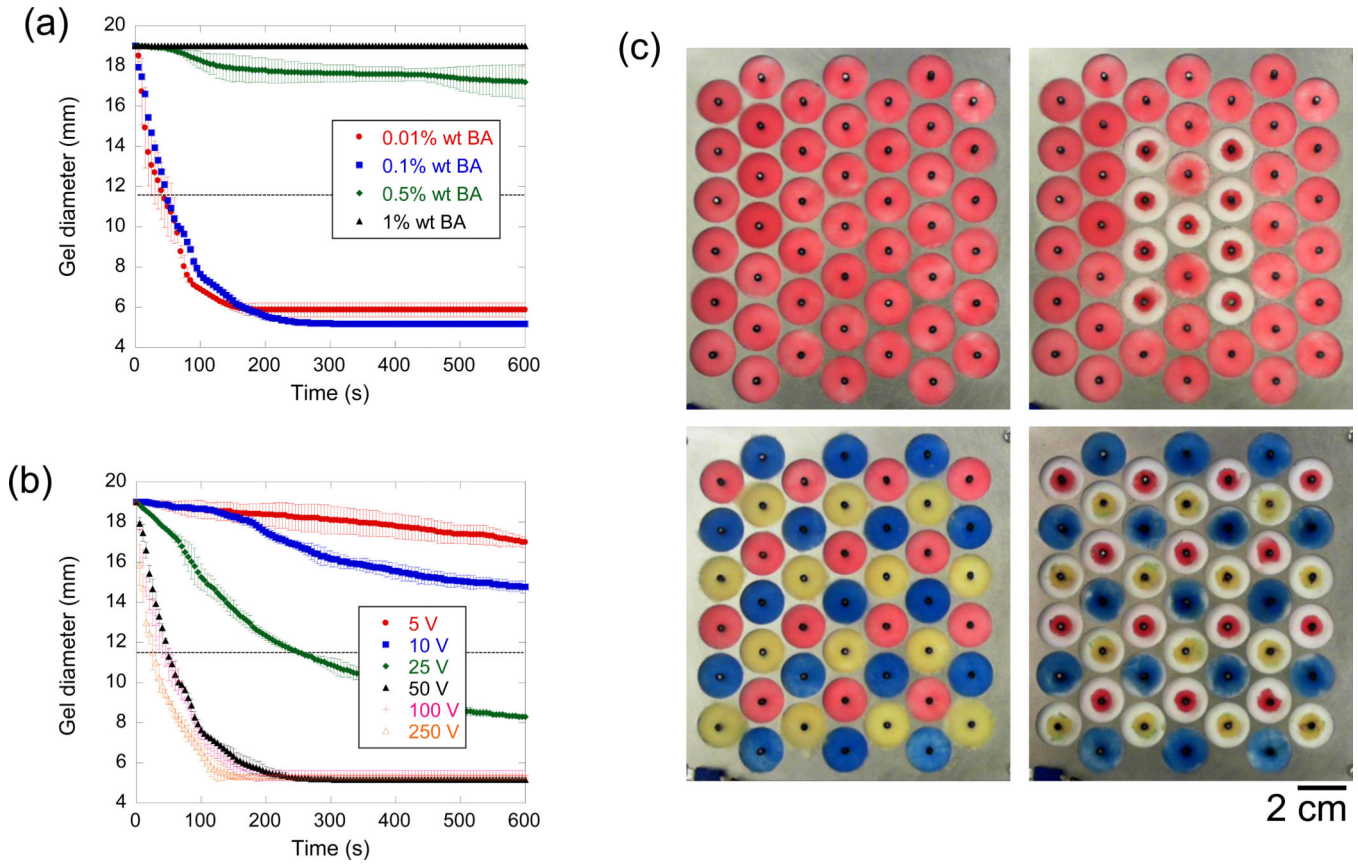

Figure 3.

Crosslinking density and applied voltage have a deterministic effect on electrical collapse, allowing dynamic arrays of gels that are individually addressed. a) Cryogel diameter is plotted versus time for gels composed of 4% wt AAc, 4% wt AAm and crosslinked at the indicated BA concentrations while exposed to 50 V in deionized water. b) Cryogel diameter is plotted versus time for gels again composed of 4% wt AAc, 4% wt AAm, crosslinked using 0.1% wt BA when exposed to the different voltages (see legend). c) An array of 4% wt AAc, 4% wt AAm cryogels, crosslinked with 0.1% wt BA was created to demonstrate the ability to easily control individual gel collapse. Both configurational (top row) and chromatic (bottom row) optical modulations were readily achieved by deciding which voltages nodes to excite (50 V for 3 min). In (a) and (b), values represent mean and standard deviation (N = 3).

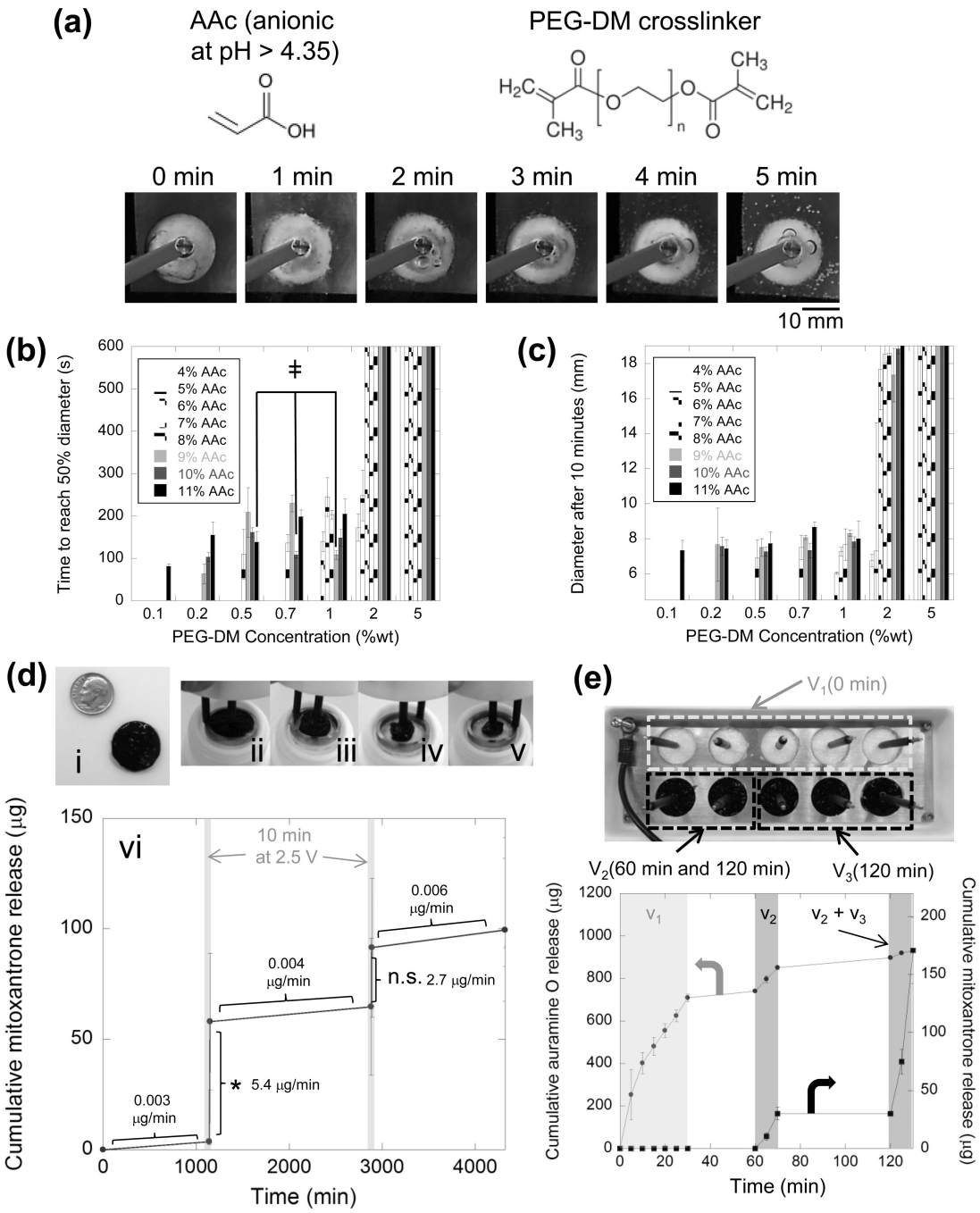

Figure 4.

Cryogels composed of polyelectrolytic, biocompatible polymer exhibit electro-responsivity and are capable of delivering drugs in a voltage-triggered manner. a) More biocompatible polyelectrolytic cryogels were created using AAc crosslinked using PEG-DM and were capable of rapid electric collapse when exposed to 50 V in deionized water. The rate (b) and extent (c) of these cryogels' electrical collapses are plotted versus the amount of AAc and PEG-DM used to construct the cryogel (see legend). ‡'s indicate gels that present a local minimum in collapse rate as AAc in increased. d) 9%wt AAc, 1% wt PEG-DM cryogels

were loaded with miotoxantrone (i) and electrically collapsed when exposed to 2.5 V in PBS (ii-v). Cumulative mitoxantrone release resulting from two 10-minute, 2.5 V pulses spaced 24 hours apart is plotted vs. time (vi). Release rates along each segment of the curve are provided on the graph and * indicates $p < 0.05$ when comparing delivery amounts before and after electrical stimulation. e) Cryogels containing two drugs (auramine O and mitoxantrone) could be integrated into arrays (top picture), from which the release profile of both drugs could be controlled with great flexibility (bottom graph). In (b) through (e), values represent mean and standard deviation ((b) and (c) N = 3, (d) and (e) N = 4).